WEP Warwick Evans Publishing

International Journal of Mechanical and Electrical Engineering

ISSN: 3005-9615 (Print), ISSN: 3005-7132 (Online) | Volume 2, Number 2, Year 2024
DOI: https://doi.org/10.62051/ijmee.v2n2.11
Journal homepage: https://wepub.org/index.php/IJMEE/index

Optimization of the Repeating Coil in Three-Coil WPT System

Boyang Yan *, Xubin Qi, Yang Yang, Kun Wang

School of Physics & Electronic Information Engineering, Henan Polytechnic University, Jiaozuo 454003, China

* Corresponding Author: Boyang Yan (Email: 1809175902@qq.com)

ABSTRACT

This paper examines the optimal conditions for the three-coil Wireless Power Transmission (WPT) system. Initially, an equivalent circuit model was developed Experiments were conducted to explore the impact of the repeating coil parameters and load resistance on the three-coil WPT system. We determined the optimal distance between the transmitting coil and the repeating resonator under various parameters of repeating coil turns, as well as different load resistance, to maximize the system's overall transmission efficiency. It indicates that in the three-coil WPT system, the optimal distance between the transmitting and repeating coils is directly proportional to the load resistance. Moreover, when the turns of the transmitting, repeating, and receiving coils are fixed at seven, the optimal distance changes slightly as the number of turns of the repeating coil increases, but changes significantly when the number of turns decreases. Additionally, when the change in load is constant, an increase in the radius of the repeating coil results in a greater change in the optimal distance. These findings provide important reference information for optimizing the efficiency of triple-coil WPT systems.

KEYWORDS

Resonant Magnetic Coupling Wireless Power Transmission; Repeating Resonator; Transmission Efficiency; Optimal Position; Three-coil System.

1. INTRODUCTION

Since the advent of wireless power transfer (WPT) technology, its convenience and efficiency have attracted considerable interest and exploration from numerous researchers. It has already demonstrated extensive potential applications in various fields such as consumer electronics [1], medical devices [2, 3], electric transportation [4-8], and outdoor equipment [9].

Many authors have established various mathematical models of WPT systems [10-12]. In article [10], the parameters of repeating coils are optimized in WPT systems through theoretical calculations and multi-objective genetic algorithms. The optimized three-coil system effectively reduces the current in the transmitting coil, enhances transmission efficiency, and minimizes electromagnetic field leakage. In ar-ticles [11, 12], a three-dimensional mathematical model of low-power periodic WPT systems is established, and geometric variant analysis is conducted on transmitting and receiving coils of different sizes and turns. Analytical formulas are utilized to ob-tain the required lumped parameters. The results demonstrate that the proposed cir-cuit model achieves similar accuracy to numerical models with significantly reduced complexity in both model and analysis.

Adding repeating coils to WPT systems further improves the transmission effi-ciency and distance, particularly suiting applications requiring higher flexibility and long-distance transmission. For WPT systems with repeating coils, there have been numerous efforts [13-15] to optimize the position of repeating coils. In article [13], achieves equal power distribution among multiple relay points through precise mathematical modeling, enhancing the efficiency of long-distance transmission signif-icantly. In article [14], the optimal position of the repeating coil is determined by an approximate expression obtained from the closed-form solution of a quintic polynomi-al equation. In article [15], an optimization design method is proposed to further en-hance the efficiency of a three-coil WPT system by adjusting the compensation capaci-tance and the position of the repeating coil.

The three-coil WPT system offers an effective balance between transmission dis-tance and system complexity. By adjusting the parameters of the repeating coil, the three-coil WPT system can accommodate various applications and environmental conditions. In article [16], an analytical expression for the compensation reactance of the repeating coil in the three-coil WPT system is derived, obtaining the optimal com-pensation reactance. The study indicates that applying the optimal compensation re-actance can improve system efficiency when the repeating coil is close to the receiving end or when the load impedance is low. Furthermore, this research investigates the ef-fects of coil positioning, load impedance, and operating frequency on system efficiency and develops a capacitor tuning method to adapt to dynamic changes in transmission distance or operating frequency. In article [17], presents an improved design for a three-coil WPT system tailored for biomedical applications. By introducing novel op-timization parameters and design methodologies, significant improvements in the transmission efficiency and performance are achieved, particularly in scenarios where the dimensions of implantable devices are constrained. In article [18], presents a three-coil WPT system with constant voltage output. This three-coil system achieves constant voltage output by setting specific coil parameter values to make the voltage gain independent of load variations, thereby realizing constant voltage output and al-leviating efficiency degradation issues during long-distance transmission. In article [19], establishes a circuit theoretical model for the three-coil WPT system and derives an analytical expression for the output current. Two operational frequencies capable of achieving load-independent output current are identified and experimentally validat-ed. In article [20], enhances the system's saturation resistance by employing a current transformer (CT) with an air-gap iron core and combines it with three-coil WPT tech-nology to achieve long-distance power transmission.

Despite numerous studies that have enhanced the performance of WPT systems with repeating coils through rigorous theoretical exploration and experimental im-provements, there is still a lack of comprehensive research on how the parameters of repeating coils specifically influence their optimal efficiency positions and the overall power transmission efficiency of the system. This study introduces repeating resonant coils with varying turns and radii into a dual-coil WPT system. Utilizing equivalent circuit theory, it investigates how the parameters of the repeating coils affect the op-timal distance between the transmitting coil and the repeating coil, under the condi-tions of fixed positions for both transmitting and receiving coils and variable load im-pedance. The findings are substantiated by experimental verification of these calcu-lated results.

2. THEORETICAL ANALYSIS

This chapter primarily presents the fundamental principles of the three-coil WPT system. The chapter is structured as follows: Section 2.1 introduces the construction of the three-coil WPT system model and calculates the system efficiency equation using Kirchhoff's voltage law (KVL) for later analysis. Section 2.2 establishes the model for a two-coil WPT system and derives its mutual inductance formula. Section 2.3 analyzes the impact of repeating coil parameter variations on mutual inductance.

2.1. Modeling and Analysis of Three-Coil WPT Systems

Figure 1 depicts the model of a three-coil WPT system, consisting of the transmitting coil, repeating coil, and receiving coil. Here, U_S represents the high-frequency AC power source, R_S is the internal resistance of the power source, R_L is the load resistance of the receiving coil, M_{12} and M_{23} denote the mutual inductances between the receiving coil and repeating coil, and between the repeating coil and receiving coil respectively. The mutual inductance between the transmitting coil and receiving coil is neglected. R_1, R_2, and R_3 are the equivalent series resistances of the coils, L_1, L_2, and L_3 represent the coil's self-inductance, C_1, C_2, C_3 and I_1, I_2, I_3 correspond to the resonant capacitance and loop current of the transmitting, repeating, and receiving coils respectively. The coils resonate at frequency f with angular resonance frequency ω, satisfying the condition:

$$\omega = 2\pi f = 1/\sqrt{L_1C_1} = 1/\sqrt{L_2C_2} = 1/\sqrt{L_3C_3} \tag{1}$$

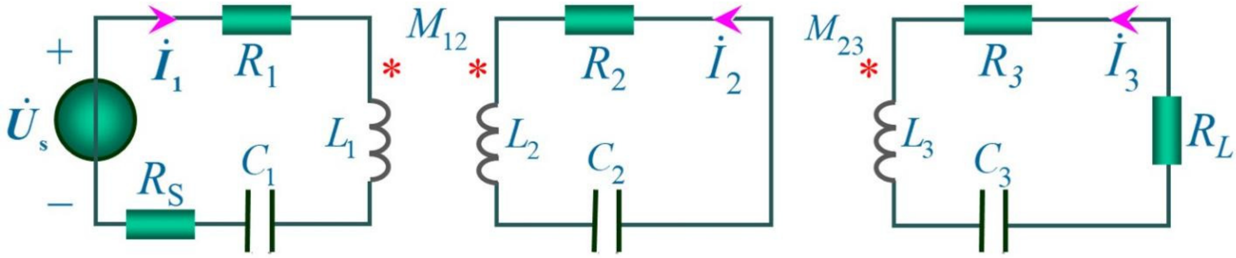

Figure 1. Model diagram of the three-coil WPT system

Assuming the total impedances of the three circuits are denoted as Z_1, Z_2, and Z_3, these parameters' values can be expressed by the following equations:

$$\begin{cases} Z_1 = R_s + R_1 + j\left(\omega L_1 - \dfrac{1}{\omega C_1}\right) \\ Z_2 = R_2 + j\left(\omega L_2 - \dfrac{1}{\omega C_2}\right) \\ Z_3 = R_L + R_3 + j\left(\omega L_3 - \dfrac{1}{\omega C_3}\right) \end{cases} \tag{2}$$

When all three coils operate in a resonant state, they achieve full resonance, and Equation (2) can be simplified to:

$$\begin{cases} Z_1 = R_s + R_1 \\ Z_2 = R_2 \\ Z_3 = R_L + R_3 \end{cases} \tag{3}$$

Based on KVL and the principle of mutual inductance coupling, we can derive the following matrix equation:

$$\begin{bmatrix} \dot{U}s \\ 0 \\ 0 \end{bmatrix} = \begin{bmatrix} Z_1 & -\mathrm{j}\omega M_{12} & 0 \\ -\mathrm{j}\omega M_{12} & Z_2 & \mathrm{j}\omega M_{23} \\ 0 & \mathrm{j}\omega M_{23} & Z_3 \end{bmatrix} \begin{bmatrix} \dot{I}_1 \\ \dot{I}_2 \\ \dot{I}_3 \end{bmatrix} \tag{4}$$

The currents in each circuit are respectively:

$$\begin{cases} \dot{I}_1 = \dfrac{\left[\omega^2 M_{23}^2 + Z_2 Z_3\right]\dot{U}_S}{\omega_0^2\left[M_{23}^2 Z_1 + M_{12}^2 Z_3\right] + Z_1 Z_2 Z_3} \\ \dot{I}_2 = \dfrac{\omega M_{12} Z_3 \dot{U}_S}{\omega^2\left[M_{23}^2 Z_1 + M_{12}^2 Z_3\right] + Z_1 Z_2 Z_3} \\ \dot{I}_3 = \dfrac{\omega^2 M_{12} M_{23} \dot{U}_S}{\omega^2\left[M_{23}^2 Z_1 + M_{12}^2 Z_3\right] + Z_1 Z_2 Z_3} \end{cases} \tag{5}$$

The load power and transmission efficiency can be calculated as follows:

$$\begin{cases} P_L = \left|\dot{I}_3\right|^2 R_L = \dfrac{\omega^4 M_{12}^2 M_{23}^2 U_s^2 R_L}{\left[\omega^2\left(M_{23}^2 Z_1 + M_{12}^2 Z_3\right) + Z_1 Z_2 Z_3\right]^2} \\ \eta = \dfrac{\left|\dot{I}_3\right|^2 R_L}{\left|\dot{U}_s \dot{I}_1\right|} = \\ \dfrac{\omega^4 M_{12}^2 M_{23}^2 R_L}{\left[\omega^2\left(M_{23}^2 Z_1 + M_{12}^2 Z_3\right) + Z_1 Z_2 Z_3\right]\left[\omega^2 M_{23}^2 + Z_2 Z_3\right]} \end{cases} \tag{6}$$

According to Equation (6), if the structural parameters of the coils are fixed, then the transmission power and efficiency of the three-coil WPT system in resonance are only related to the mutual inductances M_{12}, M_{23}, and the load R_L.

2.2. Analysis of the Mutual Inductance in a Two-coil WPT System

When the planar spiral-shaped transmit coil and the receive coil are coaxially aligned, their mutual inductance can be approximated using the following formula:

$$M_{12} = \frac{N_1 N_2 \mu_0}{4\pi} \times \oint\oint \frac{\mathrm{dl}_1 \cdot \mathrm{dl}_2}{r_{12}} \tag{7}$$

where μ_0 represents the permeability of vacuum, M_{12} denotes the mutual inductance between the transmitting coil and the receiving coil, N_1 and N_2 represent the number of turns in the transmitting and receiving coils respectively, l_1 and l_2 indicate the length of each turn in the transmitting and receiving coils, dl_1 and dl_2 correspond to the infinitesimal elements on the wires of the transmitting and receiving coils, and r_{12} represents the distance between dl_1 and dl_2. The line elements dl_1 and dl_2, and the distance r_{12} can be determined using geometric methods [21].

$$\mathrm{dl}_1 = r_1(-\sin\theta\mathbf{x} + \cos\theta\mathbf{y})d\theta \tag{8}$$

$$\mathrm{dl}_2 = r_2(-\sin\phi\mathbf{x} + \cos\phi\mathbf{y})d\phi \tag{9}$$

$$r_{12} = \left[r_1^2 + r_2^2 + \mathrm{h}^2 - 2r_1 r_2(\cos\theta\cos\phi + \sin\theta\sin\phi)\right]^{\frac{1}{2}} \tag{10}$$

where h represents the vertical distance between the transmitting and receiving coils, r_1 and r_2 respectively denote the average radius of the transmitting and receiving coils, θ and ϕ represent the temporary polar angles on the transmitting and receiving coils, and adjusting θ and ϕ allows for traversing the entire circle to complete the double integration of the transmitting and receiving coils. For clarity, Figure 2 in the following section only illustrates the case of a single turn coil.

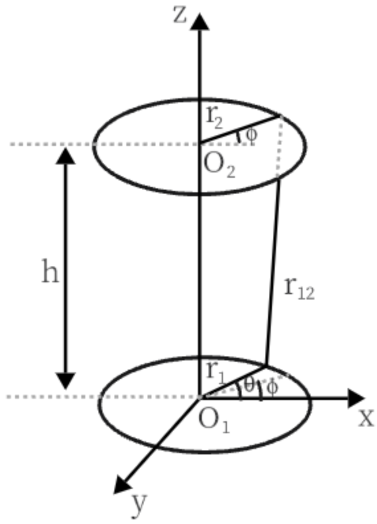

Figure 2. Diagram of the two single-turn coil WPT system model

Inserting equations (8), (9), and (10) into equation (7) yields the following result:

$$
\begin{aligned}
M_{12} = \frac{N_1 N_2 \mu_0 r_1 r_2}{4\pi} \times \oint d\phi \oint \left(\sin\theta \sin\phi + \cos\theta \cos\phi\right) \Big/ \Big[r_1^2 + r_2^2 + \mathrm{h}^2 \\
- 2 r_1 r_2 (\cos\theta \cos\phi + \sin\theta \sin\phi) \Big]^{\frac{1}{2}} d\theta
\end{aligned}
\tag{11}
$$

2.3. Analysis of the Impact of Repeating Coil Parameters on Mutual Inductance

According to equation (10), the mutual inductance between two coils is related to the radius and number of turns of the coils. When the number of turns in the transmitting coil is 7 and the radius is 10.75 cm, the relationship between the mutual inductance M_{12} between the transmitting and repeating coils and the vertical distance h is shown in Figure 3, by varying the number of turns and radius of the repeating coil.

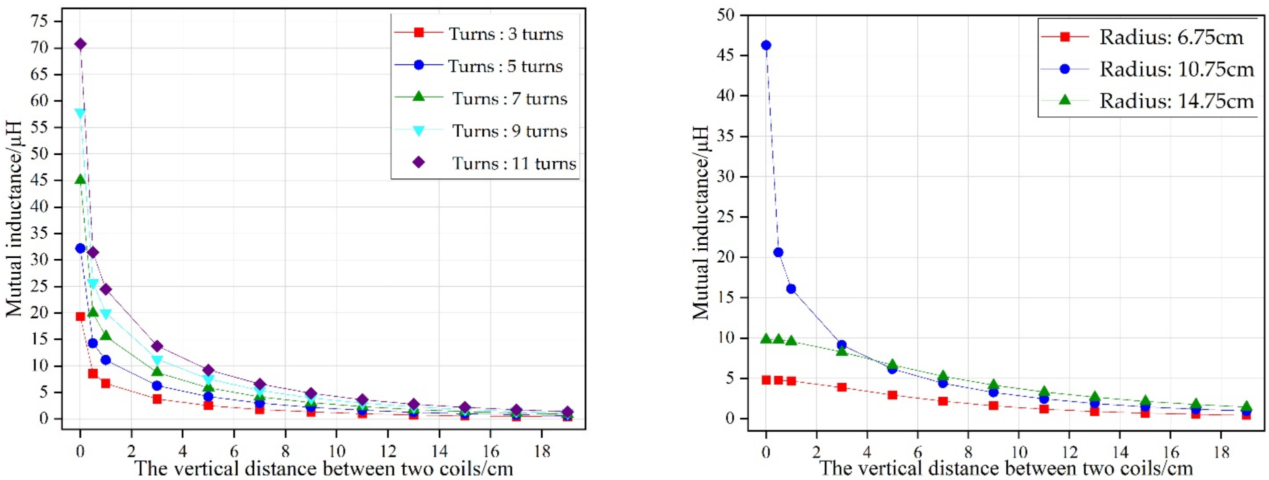

(a) **(b)**

Figure 3. Relationship between mutual inductance and the vertical distance between the two coils.: (a) Dif-ferent numbers of turns; (b) Different radii

As shown in Figure 3a, the mutual inductance M_{12} between the two coils decreases with the increase of h and the rate of decrease becomes progressively slower. When h remains constant, M_{12} is directly proportional to the number of turns in the repeating coil. As shown in Figure 3b, when the vertical distance h is less than 5 cm, the mutual inductance M_{12} with a repeating coil radius of 10.75 cm is greater than that with repeating coil radii of 6.75 cm and 14.75 cm. This is attributed to the transmitting coil having a radius of 10.75 cm. When h approaches 0 cm and the repeating coil radius is 10.75 cm, the actual distance between the wires of the transmitting and repeating coils also approaches 0 cm, leading M_{12} to tend towards infinity. Conversely, when h approaches 0 cm and the repeating coil radius is either 6.75 cm or 14.75 cm, the actual distance between the transmitting and repeating coils approaches 4 cm, and M_{12} does not trend towards infinity. For h values greater than or equal to 5 cm, M_{12} also exhibits a direct proportional relationship with the repeating coil radius. Since the parameters of the transmitting and receiving coils are identical in this study, the graphs of M_{12} and M_{23} as functions of the vertical distance h are symmetric around the line h = 10 cm.

Integrating the analysis above, it can be observed that, firstly, when h is greater than 5 cm, increasing the radius and the number of turns of the repeating coil leads to an increase in the mutual inductance between the transmitting and repeating coils. Secondly, according to equation (6), maximizing the system efficiency and power requires maximizing the product of M_{12} and M_{23}, which means M_{12} = M_{23}, achieved when h = 10 cm. However, in real-world scenarios, the impact of factors such as resistance and coil quality factors cannot be overlooked; therefore, the optimal efficiency's corresponding vertical distance h between the transmitting and repeating coils will vary around 10 cm.

3. EXPERIMENTAL ANALYSIS

In this study, an experimental platform for a three-coil WPT system was established, and mathematical calculations and simulation analyses were conducted using software. The experimental platform is illustrated in Figure 4.

The experimental setup involved obtaining electrical energy from a commercial power source of AC 220V, which was then converted into 20V DC through a DC regulated power supply. Subsequently, it was transformed into AC power of 229 kHz via a high-frequency inverter for supply to the transmitting coil. The energy was transmitted through the repeating coil to the receiving coil, with all coils made of high-frequency enameled wire (0.1 mm × 160 strands) and aligned along the same axis. The load connected to the receiving coil comprised cement resistors of varying resistance values, and data collection was accomplished by monitoring the voltage at the receiving end using an oscilloscope. The key parameters of the system circuit are detailed in Tables 1 and 2.

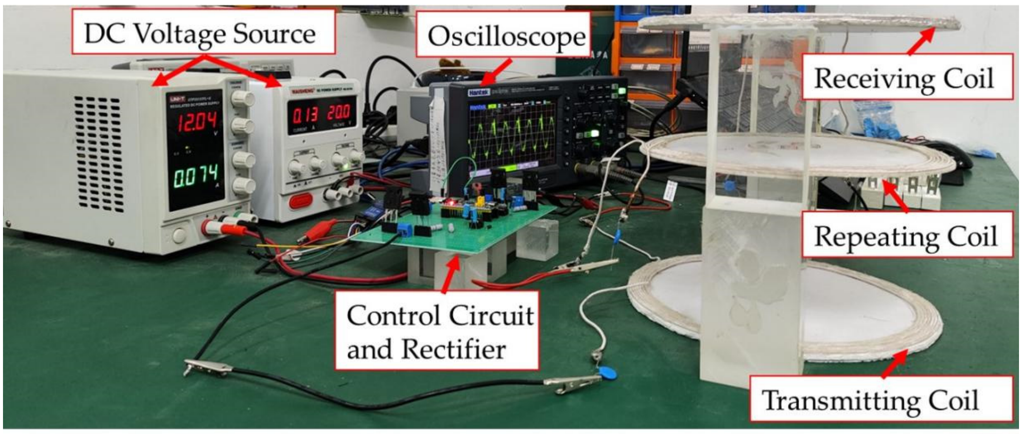

Figure 4. Experimental Platform of Three-Coil WPT System

Table 1. Parameters of the WPT system

Note	Symbol	Value
Transmitting coil inductance	L_1	22[μH]
Transmitting coil resonant capacitor	C_1	22[nF]
Receiving coil inductance	L_2	22[μH]
Receiving coil resonant capacitor	C_2	22[nF]
Input voltage	U_S	20[V]
Resonance frequency	f	229[kHz]

Subsequently, we will examine the relationship between the energy transmission efficiency of the three-coil WPT system and the position of the repeating coil when the number of turns and radius vary. The number of turns, radius, self-inductance (L_C), and resonant capacitance (C_C) for repeating coils 1-7 are detailed in Table 2. The transmitting and receiving coils are depicted in Figure 5, each with 7 turns and a radius of 10.75 cm. Repeating coils with different numbers of turns are shown in Figure 6a, where repeating coils 1, 2, 4, and 5 have a radius of 10.75 cm and turns of 3, 5, 9, and 11, respectively. Repeating coils with different radii are presented in Figure 6b, where repeating coils 6, 3, and 7 have 7 turns and radii of 14.75 cm, 10.75 cm, and 6.75 cm, respectively.

Figure 5. Transmitting and receiving coils

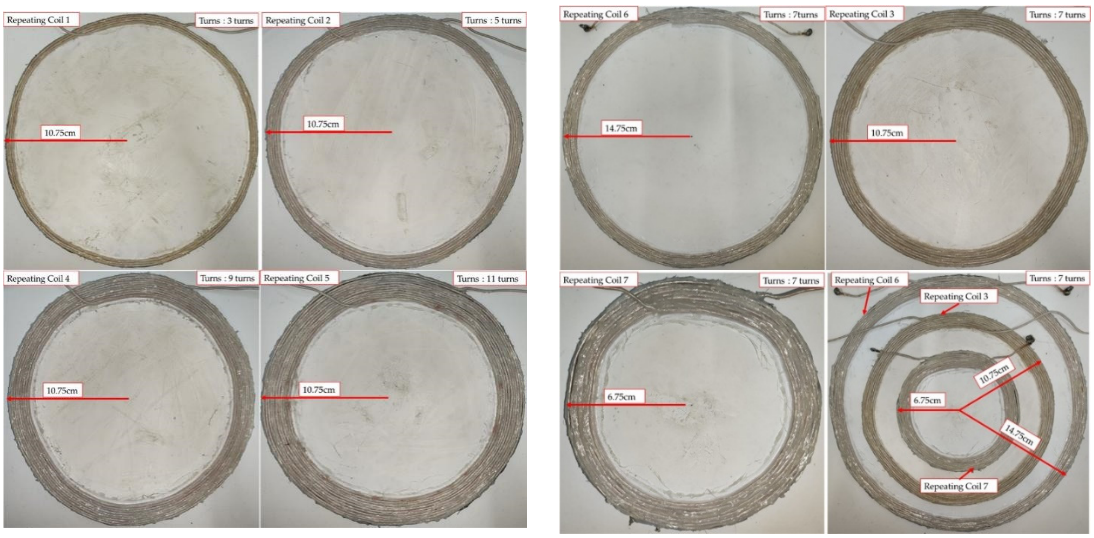

(a) **(b)**

Figure 6. Repeating coils of different turns and radii: (a) Different numbers of turns; (b)Different radii

Table 2. Measured lumped parameters of repeating coils and compensation capacitors

No.	Turns	Radius [cm]	L_C [μH]	C_C [nF]
1	3	10.75	7	69
2	5	10.75	15	32
3	7	10.75	22	22
4	9	10.75	36	13
5	11	10.75	43	11
6	7	14.75	37	13
7	7	6.75	12	40

Figure 7 illustrates the relationship between the load resistance R_L, the distance h between the transmitting coil and the repeating coil, and the transmission efficiency when the number of turns in the transmitting, repeating, and receiving coils is 7, and their radii are all 10.75 cm.

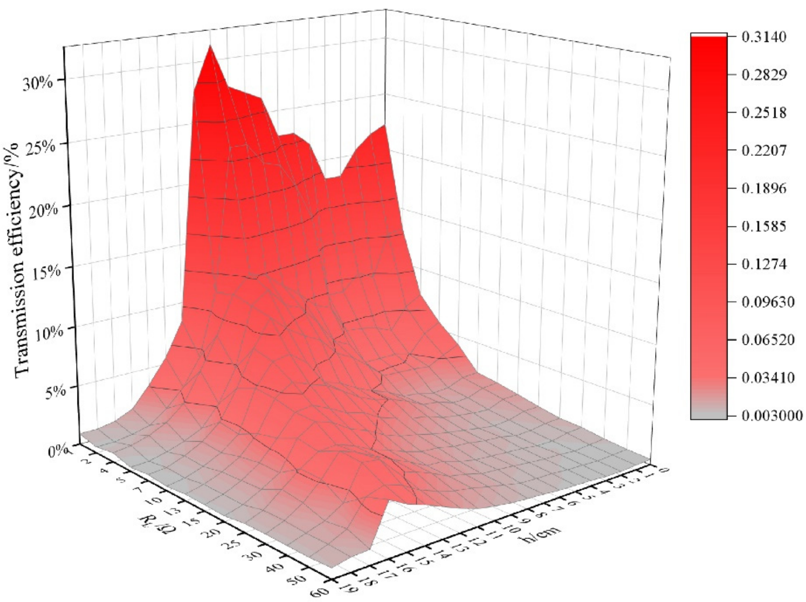

Figure 7. The Relationship between h, R_L, and Efficiency.

The system is driven by an inverter circuit powered by a DC regulated power supply, providing adjustable high-frequency AC power. Its circuit properties are different from those of high-frequency AC power sources, and variations in the position of the repeating coil have very little impact on the output power of the DC regulated power supply. Therefore, in the simulation calculations, we utilized the load power from equation (6) as the source of simulated data and calculated the transmission efficiency based on constant input power. In Figure 7, the distance between the transmitting and receiving coils is maintained at 20 cm, where h represents the distance between the transmitting and repeating coils. Maintaining R_L constant and h greater than 5 cm, we observe that as h increases, transmission efficiency initially increases and then decreases, reaching a maximum value at a certain h value. When R_L is relatively small, the h value corresponding to the maximum transmission efficiency is close to 10 cm. As R_L increases, the h value corresponding to the maximum transmission efficiency also increases, and the maximum value of transmission efficiency decreases with the increase in R_L. When h is less than 5 cm, as h increases, the value of transmission efficiency decreases. This is because when the actual distance between the transmitting coil and the repeating coil approaches 0 cm, their mutual inductance increases rapidly. In summary, the experimental data validate the theoretical analysis presented in Section 2.3. When interference from resistance is minimal, the optimal efficiency corresponds to an h value around 10 cm. With an increase in resistance, the h value corresponding to the optimal efficiency also increases.

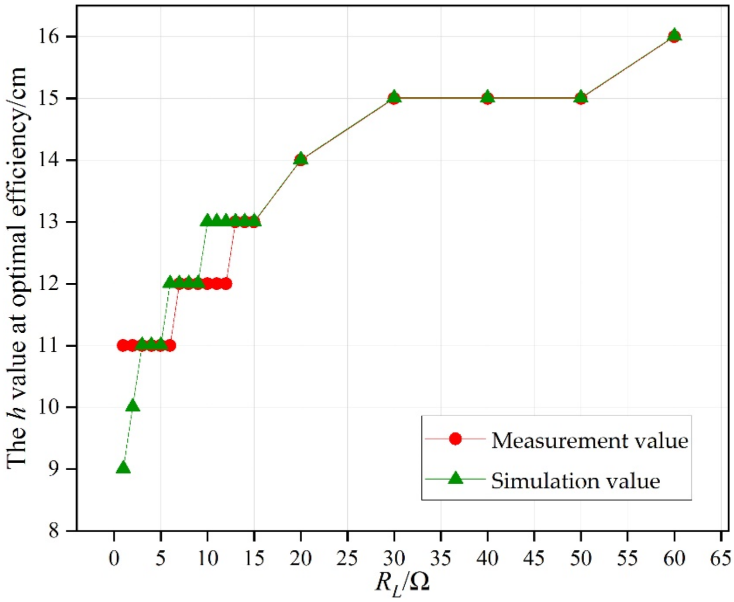

Figure 8. The Relationship between h and R_L at Optimal Efficiency

The simulation calculations were performed by incorporating Equations (6) and (11). The number of turns for the transmission, repeating, and receiving coils was set to 7 each with a radius of 10.75 cm. The relationship between the value of h at the optimal efficiency and the load resistance R_L is shown in Figure 8. In Figure 8, there is a proportional relationship between the optimal efficiency state of h and the load resistance R_L. The trend variation between the simulation results and experimental measurements is essentially consistent. The reason for the incomplete consistency between simulation and experiment lies in the assumption of ideal coils in the simulation, which neglects the energy loss of the coils. The energy loss of the coils is influenced by their winding method. Therefore, simulation and experiment may not be entirely consistent. If the energy loss of the coils is excessively high, the difference between the two could be considerable.

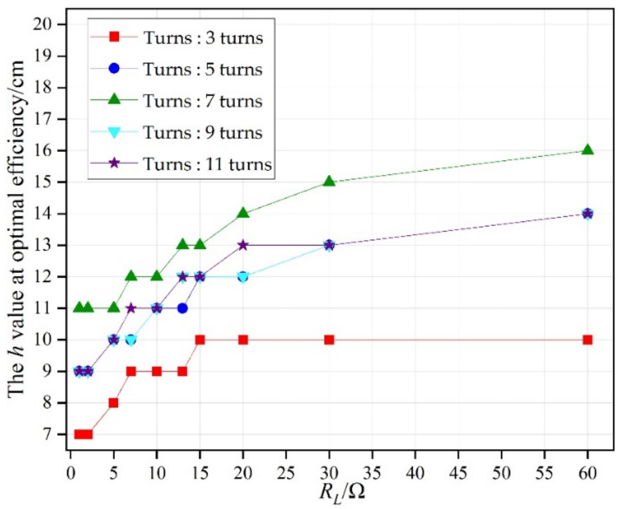

Figure 9. Relationship between h and R_L at the Best Efficiency when the Repeating Coil has 3-11 Turns

Under lower R_L resistance values, the variation of h at the optimal efficiency state is rapid, and the experimental measurement data is more densely concentrated. As R_L further increases, the growth trend of h at the optimal efficiency slows down, accompanied by a corresponding increase in the spacing of experimental measurement data. When R_L is low, the value of h at the optimal efficiency is close to half the distance between the transmission coil and the receiving coil, i.e., 10 cm. As R_L increases, the value of h at the optimal efficiency gradually moves toward the receiving coil direction from 10 cm.

As shown in Figure 9, the relationship between the load resistance R_L and the vertical distance h at optimal efficiency is plotted for setups where all coil radii are uniformly 10.75 cm, with the transmitting and receiving coils consisting of 7 turns each, and the repeating coils varying in turns of 3, 5, 7, 9, and 11 respectively. As the number of turns of repeating coil varies, the load resistance R_L exhibits a positive correlation with the vertical distance h at optimal efficiency. Specifically, when the number of turns for the repeating coil, the transmitting and receiving coils, is uniformly 7, the vertical distance h at optimal efficiency is consistently highest across different R_L values. Using a repeating coil with 7 turns as a reference, the reduction in the number of turns has a significantly greater impact on the vertical distance h at optimal efficiency compared than increasing the number of turns. Specifically, while the change in h is minimal when the number of turns is increased from 9 to 11, a notable decrease in h at optimal efficiency is observed when the number of turns is reduced from 5 to 3. This decrease can be attributed to the lower quality factor of the 3-turn coil, which results in increased energy loss. Therefore, the number of turns in the coil should not be too high, as an excessive number can lead to increased coil resistance and greater energy loss. Conversely, the number of turns should not be too low either, since a reduced number of turns can result in lower self-inductance, thereby decreasing the quality factor and increasing the rate of energy dissipation.

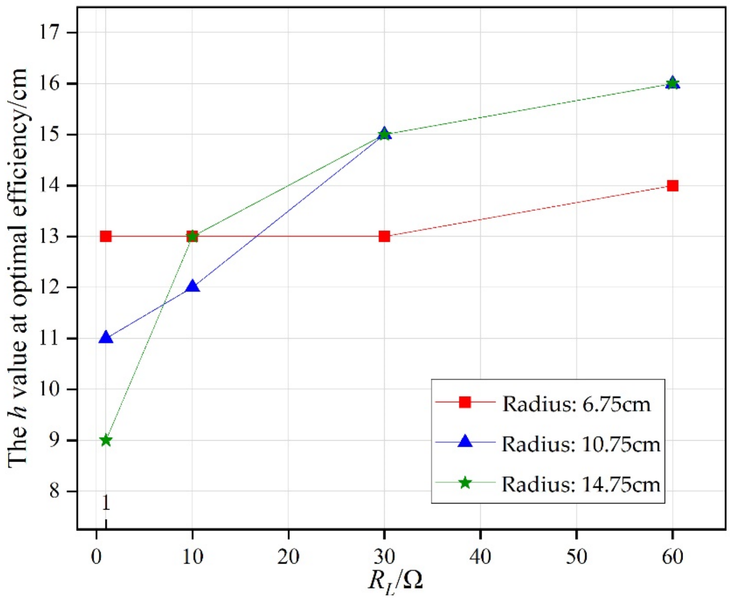

Figure 10. The Relationship between h and R_L at Optimal Efficiency under Different Repeating Coil Radii

As shown in Figure 10, the relationship between the load resistance R_L and the vertical distance h at optimal efficiency is shown for configurations where the transmitting, repeating, and receiving coils each have 7 turns. The radii of the transmitting and receiving coils are 10.75 cm and the radius of the repeating coil varies at 6.75 cm, 10.75 cm, and 14.75 cm respectively. Under different repeating coil radii, the load resistance R_L shows a positive correlation with the vertical distance h at optimal efficiency. For 6.75 cm repeating coil radius, as the load resistance changes from 1 ohm to 60 ohms, the h value at optimal efficiency remains relatively stable. For repeating coil radii of 10.75 cm and 14.75 cm, as the load resistance varies from 1 ohm to 60 ohms, the h value at optimal efficiency experiences more significant fluctuations. Furthermore, when the load resistance exceeds 30 ohms, the h values at optimal efficiency tend to converge for both 10.75 cm and 14.75 cm radii. Observing the variations in the vertical distance h at optimal efficiency for load resistances of 1 ohm and 60 ohms across different repeating coil radii, it can be seen that the difference in h values increases with the radius of the repeating coil. Specifically, a larger repeating coil radius results in a greater sensitivity of the h value to changes in load, due to the fact that a smaller coil radius reduces the magnetic field coverage, thus hindering effective coupling with transmitting or receiving coils at greater distances.

4. CONCLUSION

This paper investigates how the number of turns and the radius of the relay coil affect the efficiency of power transmission in a three-coil WPT system. After fixing the positions of the transmitting resonant coil and the final receiving coil, the optimal distance between the transmitting and relay coils was observed. Experiments were repeatedly conducted with multiple adjustments to the load resistance values. Analysis of the experimental data trends revealed that the resistance load values are directly proportional to the optimal distance between the transmitting coil and the relay coil under peak system efficiency. Additionally, when the number of turns in the relay coil equals that of the transmitting and receiving coils, and the load resistance varies, the optimal distance between the transmitting and relay coils consistently exceeds the distances when the relay coil's number of turns differs from those of the transmitting and receiving coils. Furthermore, it was discovered that an increase in the radius of the relay coil leads to a greater sensitivity of the optimal distance between the transmitting and relay coils to changes in load. This analysis provides critical reference for efficiency optimization in the three-coil WPT system.

CONFLICTS OF INTEREST

Boyang Yan proposed the main idea, Boyang Yan and Xubin Qi performed the experiments, and together they wrote the manuscript. Boyang Yan, Yang Yang, and Kun Wang double-checked the results and the entire manuscript. All authors have approved the final version of this manuscript.

ACKNOWLEDGMENTS

This research was funded by the Doctoral Fund Project of Henan Polytechnic University（B2014-028）.

REFERENCES

[1] Park, J.; Kim, D.; Hwang, K.; Park, H.H.; Kwak, S.I.; Kwon, J.H.; Ahn, S. A Resonant Reactive Shielding for Planar Wireless Power Transfer System in Smartphone Application[J]. IEEE Trans. Electromagn. Compat. 2017, 59, 695-703. [CrossRef]

[2] Alshhawy, S.; Barakat, A.; Yoshitomi, K.; Pokharel, R.K. Compact and Efficient WPT System to Embedded Receiver in Biological Tissues Using Cooperative DGS Resonators [J]. IEEE Trans. Circuits Syst. II-Express Briefs. 2022, 69, 869-873. [CrossRef]

[3] Kiani, M. Wireless Power Transfer and Management for Medical Applications: Wireless power [J]. IEEE Solid-State Circuits Mag. 2022, 14, 41-52. [CrossRef]

[4] Sun, L.; Ma, D.; Tang, H. A review of recent trends in wireless power transfer technology and its applications in electric vehicle wireless charging. Renew. Sustain. Energy Rev. 2018, 91, 490–503. [CrossRef]

[5] Luo, Z.; Wei, X. Analysis of Square and Circular Planar Spiral Coils in Wireless Power Transfer System for Electric Vehicles. IEEE Trans. Ind. Electron. 2018, 65, 331–341. [CrossRef]

[6] Batra, T.; Schaltz, E.; Ahn, S. Effect of ferrite addition above the base ferrite on the coupling factor of wireless power transfer for vehicle applications. J. Appl. Phys. 2015, 117, 17D517. [CrossRef]

[7] Inoue, K.; Kusaka, K.; Itoh, J.I. Reduction in radiation noise level for inductive power transfer systems using spread spectrum techniques. IEEE Trans. Power Electron. 2018, 33, 3076–3085. [CrossRef]

[8] Zhai, L.; Zhong, G.; Cao, Y.; Hu, G.; Li, X. Research on Magnetic Field Distribution and Characteristics of a 3.7 kW Wireless Charging System for Electric Vehicles under Offset. Energies. 2019, 12, 392. [CrossRef]

[9] Stankiewicz, J.M.; Steckiewicz, A.; Choroszucho, A. Analysis of Simultaneous WPT in Ultra-Low-Power Systems with Multiple Resonating Planar Coils. Energies. 2023, 16, 4597. [CrossRef]

[10] Wen, F.; Chu, X.; Li, Q.; Li, R.; Liu, L.; Jing, F. Optimization on Three-Coil Long-Range and Dimension-Asymmetric Wireless Power Transfer System. IEEE Trans. Electromagn. Compat. 2020, 62, 1859-1868. [CrossRef]

[11] Steckiewicz, A.; Stankiewicz, J.M.; Choroszucho, A. Numerical and Circuit Modeling of the Low-Power Periodic WPT Systems. Energies. 2020, 13, 2651. [CrossRef]

[12] Stankiewicz, J.M. Evaluation of the Influence of the Load Resistance on Power and Efficiency in the Square and Circular Periodic WPT Systems. Energies. 2023, 16, 2950. [CrossRef]

[13] Lu, F.; Zhang, H.; Li, W.; Zhou, Z.; Zhu, C.; Cheng, C.; Deng, Z.; Chen, X.; Mi, C.C. A High-Efficiency and Long-Distance Power-Relay System with Equal Power Distribution. IEEE J. Emerg. Sel. Top. Power Electron. 2020, 8(2): 1419-1427. [CrossRef]

[14] Reddy, G.K.; Mishra, D.; Devi, L.N. Optimal Relay Coil Placement in Magnetic Resonant Coupling-Based Power Transfer. IEEE Commun. Lett. 2021, 25(9): 2874-2878. [CrossRef]

[15] Liu, X.; Song, X.; Yuan, X. Compensation Optimization of the Relay Coil in a Strong Coupled Coaxial Three-Coil Wireless Power Transfer System. IEEE Trans. Power Electron. 2022, 37, 4890-4902. [CrossRef]

[16] Wang, Q.; Wang, Y. Power efficiency optimisation of a three-coil wireless power transfer using compensatory reactance. IET Power Electron. 2018, 11, 2102-2108. [CrossRef]

[17] Machnoor, M.; Gámez Rodríguez, E.S.; Kosta, P.; Stang, J.; Lazzi, G. Analysis and Design of a 3-Coil Wireless Power Transmission System for Biomedical Applications. IEEE Trans. Antennas Propag. 2019, 67, 5012-5024. [CrossRef]

[18] Souza, K.N.; Pontes, R.S.T.; Oliveira, A.P.; Barreto, G.A. Design and Control of a Three-Coil Permanent Magnet Spherical Motor. Energies. 2018, 11, 2009. [CrossRef]

[19] Sun, L.; Tang, H.; Zhang, Y. Determining the Frequency for Load-Independent Output Current in Three-Coil Wireless Power Transfer System. Energies. 2015, 8, 9719-9730. [CrossRef]

[20] Li, W.; Chen, Y.; Peng, Z.; Wang, X.; Xia, C. Investigation on Induced Energy Extraction from High-Voltage Transmission Lines Based on Three-Coil WPT Systems. Energies. 2023, 16, 3079. [CrossRef]

[21] Liu, F.; Yang, Y.; Jiang, D.; Ruan, X.; Chen, X. Modeling and Optimization of Magnetically Coupled Resonant Wireless Power Transfer System with Varying Spatial Scales. IEEE Trans. Power Electron. 2017, 32(4): 3240-3250. [CrossRef]